Available online at www.eccomasproceedia.org
Eccomas Proceedia COMPDYN (2017) 5056-5069

ECCOMAS Proceedia

COMPDYN 2017
6th ECCOMAS Thematic Conference on
Computational Methods in Structural Dynamics and Earthquake Engineering
M. Papadrakakis, M. Fragiadakis (eds.)
Rhodes Island, Greece, 15–17 June 2017

ADVANCED NUMERICAL MODELS FOR THE ANALYSIS OF UNREINFORCED AND STRENGTHENED MASONRY VAULTS

V.P. Berardi, M. De Piano, G. Teodosio, R. Penna, L. Feo
University of Salerno, Department of Civil Engineering
84084, Fisciano, SA, Italy
e-mail: berardi@unisa.it, mdepiano@unisa.it, g.teodosio@studioteodosio.it, rpenna@unisa.it, l.feo@unisa.it

Keywords: Masonry structures, Genetic algorithm, Adaptive finite element model, Strengthening, Composite materials

Abstract. *Masonry buildings realized in the last centuries are a significant part of the international architectural heritage. The optimal design of the retrofit interventions of these buildings represents a priority and requires the evaluation of their mechanical behavior under static and dynamic loads. Several mechanical models capable to study masonry structures are available in literature and are based on Heyman limit analysis approach. These models cannot be easily adopted within FEM codes. Within this context, a Genetic Algorithm is implemented within a refinement adaptive finite element model to computational mesh of shell surfaces. The proposed model researches a 'safe' thrust surface of a masonry vault within a design domain, by minimizing the average value of the principal tensile stresses carried by the unreinforced portion of the material (fitness function). The design domain coincides with either the vault volume, in the case of unreinforced masonry members, or an external region of the vault in correspondence with the reinforced portions, in the case of the vault strengthened with either Fiber Reinforced Polymer or Fabric Reinforced Cementitious composites. The proposed methodology allows evaluating the structural safety of masonry vault and defining an optimal design of reinforcement pattern.*

Peer-review under responsibility of the organizing committee of COMPDYN 2017.
doi: 10.7712/120117.5784.17716

1 INTRODUCTION

Nowadays, the safeguard of masonry historical constructions represents an international priority. The evaluation of structural vulnerability of these constructions is the first step to evaluate their safe and to preserve them over time by means of retrofit/strengthening interventions.

Several mechanical models available in literature are based on either local failure mechanisms [1]-[5] or the Heyman limit analysis approach [6]. With reference to curved structures, the safe theorem of Heyman has been used to via either continuous [7]-[10] or discontinuous [11]-[15] approaches. The theoretical approach and the computational burden of such models makes non easy their implementation in FEM code.

In the recent years, structural optimization problems have been examined by means of genetic/evolutionary algorithms (GA), inspired by Darwin's evolution theory [16]-[19].

This paper presents an advanced numerical model capable to search a ‘safe’ thrust surface of masonry vaults. It is based on a Breeder Genetic Algorithm (BGA) proposed by the authors in previous studies and applied to a FEM approximation of the vault geometry via shell elements [20]. The BGA allows to find a safe thrust surface by moving the FEM nodes of a vault within a design domain and minimizing the average value of the principal tensile stresses in unreinforced masonry. The model can be also adopted to the design the vaults strengthened with fiber reinforced cementitious matrix (FRCM) composites. Numerical results are given for a cloister vault subject to static and dynamic load combinations.

2 NUMERICAL MODEL

The proposed numerical procedure is formulated within the field of linear elasticity. We model the masonry framework through a FEM approximation, by using shell elements with dominant membrane behavior (Figure 1).

Let denote the i-th coordinate of the j-th node, $x_{i,j}$; the lower bound of $x_{i,j}$ (corresponding to the intrados of the vault for unreinforced masonry), $x_{i,j}^{min}$; the upper bound of $x_{i,j}$ (corresponding to the extrados of the vault for unreinforced masonry), $x_{i,j}^{max}$; control variables ranging in the interval [0,1], $\xi_{i,j}$.

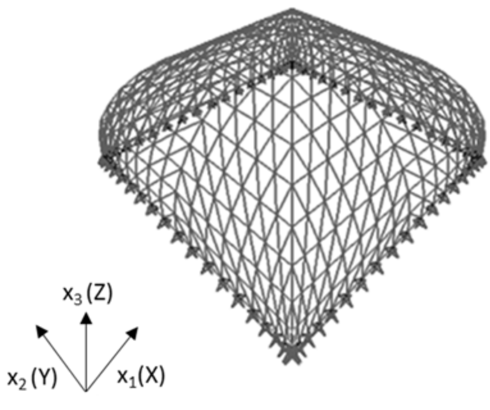

Figure 1: FEM modelling of vaults

We search a safe thrust surface of vaults by moving FEM nodes within a design domain, expressed as follows:

$$x_{i,j} = x_{i,j}^{min} + \xi_{i,j}\left(x_{i,j}^{max} - x_{i,j}^{min}\right) . \tag{1}$$

The search of the safe thrust surface is performed through the BGA [21], by minimizing the fitness function corresponding to the average value of the principal tensile stresses in unreinforced masonry.

More specifically, if we assume n and N (=3 n if all the 3 nodal coordinates govern the r-adaptation strategy) are the total number of the FEM nodes and the control variables $\xi_{i,j}$, respectively, we can introduce the m-th "individual" corresponding to the t-th generation:

$$x_m^t = (x_{1,1}, \dots \dots, x_{3,n})_m . \tag{2}$$

The BGA find the safe thrust surface by performing the following steps [20]:

1. an initial population of λ individuals is generated;
2. the μ best individuals are selected within the current population of λ elements;
3. the best individual is retained for the next generation;
4. the remaining λ-1 individuals of the next generation are created by means of the Extended Intermediate Recombination (EIR)[22] and mutation the μ best individuals of the current generation;
5. Steps 2 through 4 are repeated until the value of fitness function is less than a fixed value.

The proposed procedure allows us to approximate the elastic no-tension constitutive model of unreinforced masonry within a linear elastic FEM analysis [7]-[15].

3 CASE STUDY

We analyze the case study of a tuff masonry cloister vault (Figure 2) subject to static and dynamic loads.

The cloister vault, as well known, is generated by the intersection more barrel vaults set on opposite sides of a base polygon. The stress state in this kind of vault is more complex than that exhibited by groin and barrel vaults.

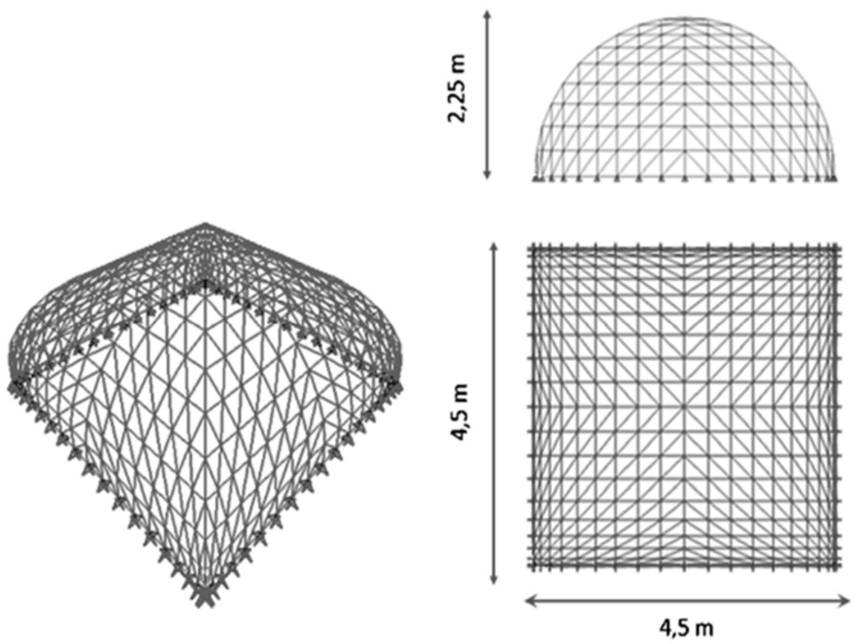

Figure 2: 3D, front and top views of the finite element modelling

The examined vault is characterized by the constant thickness of 0,25 m and its geometry is depicted in Figure 3.

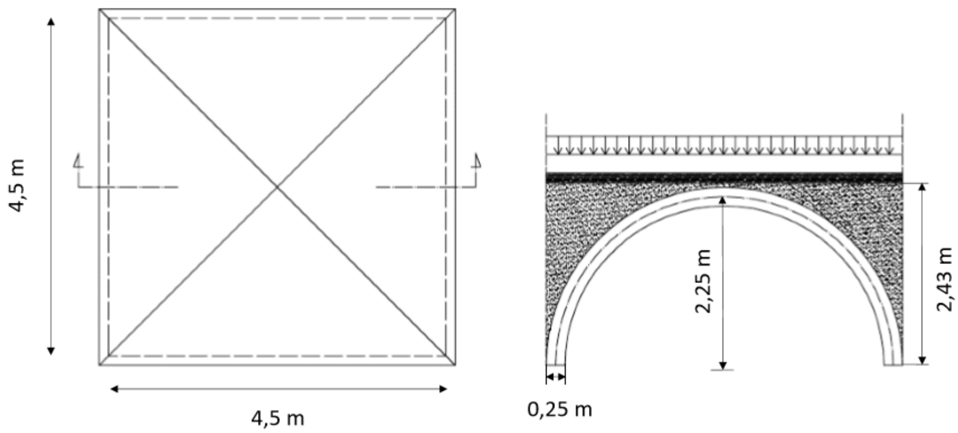

Figure 3: Plan and section of the cloister vault.

The masonry framework is modeled by means of the CSI SAP90 FEM software. The mesh consists of 441 nodes and 800 triangular shell elements with dominant membrane behavior, since bending thickness is fixed equal to 1/5 of the membrane thickness.

We assumed the physical and mechanical properties of the materials, reported in Table 1 (γ_1 = specific weight of masonry, γ_2 = specific weight of filling material, E_m = Young modulus of masonry). The basis of the cloister vaults is restrained by fixed hinge supports.

We consider two static case studies: cloister vault subject to its self-weight; cloister vault subject to the dead and live loads.

We also examine the vault under the load combination obtained by vertical and seismic loads. The seismic action is modeled according to static approach suggested in European Standard EN 1998-1 [23].

γ_1 [kN/m^3]	γ_2 [kN/m^3]	E_m [MPa]
15,00	10,00	1500,00

Table 1: Physical and mechanical properties of the materials.

Finally, we propose an optimized strengthening intervention with FRCM composites of the vault.

We denote 'RTS' the Reference Thrust Surface corresponding to the midsurface of the cloister vault, 'MTTS' the Minimum Tension Thrust Surface obtained via the proposed numerical procedure.

Within numerical simulations, the fitness function is applied to unreinforced masonry; the relocating of FEM nodes of the unstrengthened masonry is allowed along the *Z*-axis of the Cartesian frame within the vault volume [20].

Plots of maximum and minimum principal axial internal forces are given in the following, referred to the RTS and the MTTS.

3.1 Self-weight

Firstly, we apply the numerical model to the vault subject to its self-weight. Starting from the FEM analysis on the RTS and the MTTS (Figure 4), the maximum and minimum internal axial forces acting on midsurface of shell elements are obtained (Figure 5).

In terms of local stresses, the maximum and minimum principal stresses on the RTS are equal to $\sigma_{max} = 3{,}04 \times 10^{-2}$ MPa and $\sigma_{min} = -4{,}40 \times 10^{-2}$ MPa, respectively, as well as the average value of the tensile principal stresses is equal to $\sigma_{ave} = 3{,}73 \times 10^{-9}$ MPa.

The results obtained by considering the MTTS highlight the maximum principal stress ($\sigma_{max} = 8{,}24 \times 10^{-4}$ MPa) and the average value of the tensile principal stresses ($\sigma_{ave} = 5{,}35 \times 10^{-10}$ MPa) are significantly smaller than that obtained by the RTS, and the minimum principal compressive stress given by the MTTS ($\sigma_{min} = -4{,}08 \times 10^{-2}$ MPa) is almost unchanged compared to that given by the RTS.

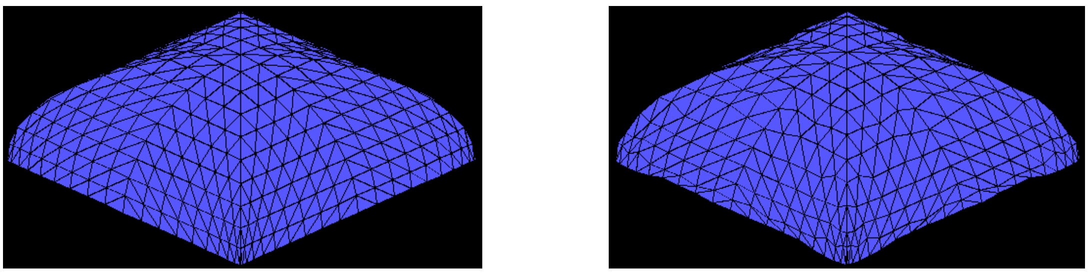

Figure 4: RTS and MTTS configurations.

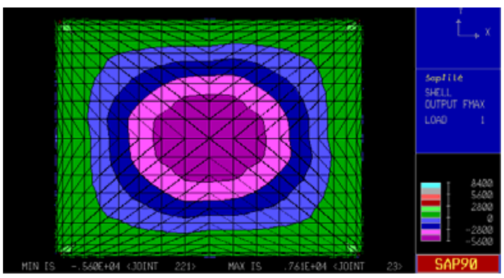

RTS: maximum principal internal forces [N/m]

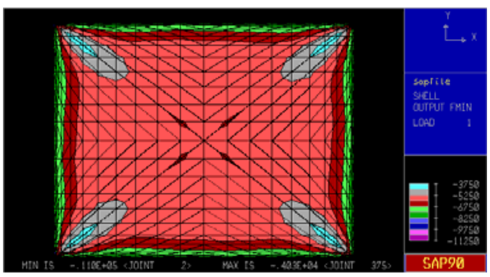

RTS: minimum principal internal forces [N/m]

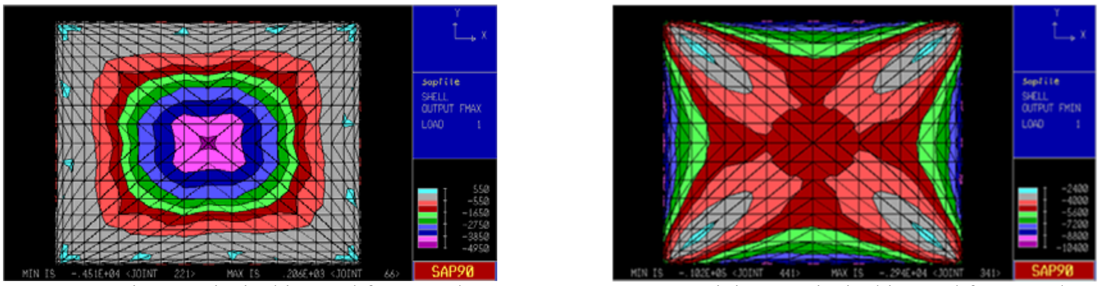

MTTS: maximum principal internal forces [N/m] MTTS: minimum principal internal forces [N/m]

Figure 5: Top views of the unreinforced vault subject to its self-weight.

3.2 Dead and live loads

Let us examine the vault subject to the following static design load combination, LC_{St}:

$$\boldsymbol{LC_{St}} = \boldsymbol{G_1} + \left(\boldsymbol{G_{2,1}} + \boldsymbol{G_{2,2}}\right) + \boldsymbol{Q} \tag{3}$$

where:
G_1 is the dead load due to the self-weight of the vault;
$G_{2,1}$ is the dead load due to the weight of the filling material;
$G_{2,2}$ is the dead load due to the permanent overload and it is assumed equal to 3,00 kN/m^2;
Q is the live load ad it is fixed equal to 4,00 kN/m^2.

The FEM analysis on the RTS and the MTTS (Figure 6) gives the maximum and minimum internal axial forces acting on midsurface of shell elements (Figure 7).

The corresponding maximum and minimum principal stresses on the RTS are equal to $\sigma_{max} = 1.03 \times 10^{-1}$ MPa and $\sigma_{min} = -1{,}40 \times 10^{-1}$ MPa, respectively, as well as the average value of the tensile principal stresses is equal to $\sigma_{ave} = 1{,}26 \times 10^{-8}$ MPa.

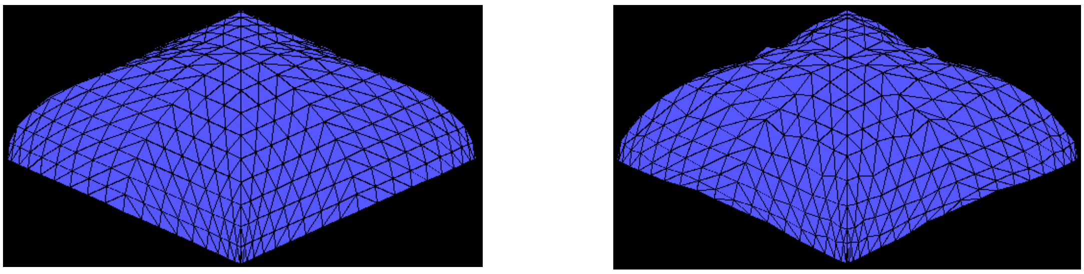

Figure 6: RTS and MTTS configurations

The MTTS allows to point out the maximum principal stress ($\sigma_{max} = 7{,}20 \times 10^{-3}$ MPa) and the average value of the tensile principal stresses ($\sigma_{ave} = 3{,}01 \times 10^{-9}$ MPa) are significantly smaller than that obtained by the RTS, and the minimum principal compressive stress given by the MTTS ($\sigma_{min} = -1{,}42 \times 10^{-1}$ MPa) remains almost unchanged in magnitude compared to that given by the RTS.

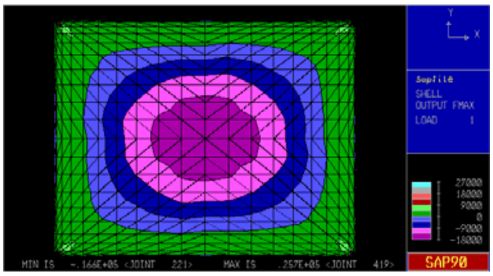

RTS: maximum principal internal forces [N/m]

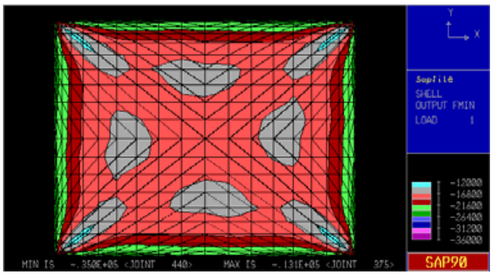

RTS: minimum principal internal forces [N/m]

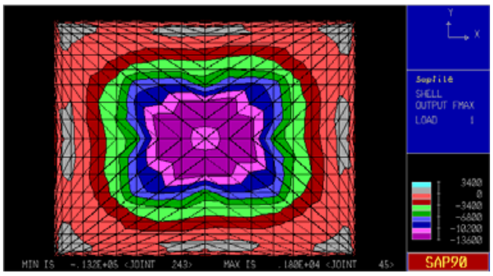

MTTS: maximum principal internal forces [N/m]

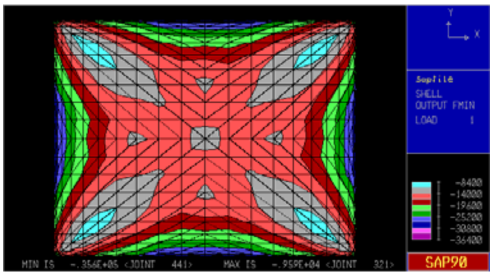

MTTS: minimum principal internal forces [N/m]

Figure 7: Top views of the unreinforced vault subject to dead and live loads.

3.3 Seismic loads and strengthening with FRCM strips

Let us examine the vault subject to the following dynamic design load combination, LC_{Dyn}:

$$\boldsymbol{LC_{Dyn} = E + G_1 + \left(G_{2,1} + G_{2,2}\right) + \psi_{2,1} Q} \tag{4}$$

where:
E is the load due to the seismic excitation along the *X*-axis of the Cartesian frame (Figure 8);
G_1 is the dead load due to the self-weight of the vault;
$G_{2,1}$ is the dead load due to the weight of the weight of filling material;
$G_{2,2}$ is the dead load due to the permanent overload and it is assumed equal to 3,00 kN/m^2;
$\psi_{2,1}$ is the combination coefficient and it is assumed equal to 0,80;
Q is the live load ad it is fixed equal to 4,00 kN/m^2.

The effects of the seismic excitations are modeled by means of horizontal forces according to a conventional static approach to seismic actions on the buildings (European Standard EN 1998-1). The seismic forces are set 50% of the vertical forces.

The maps of the maximum and minimum internal axial forces acting on midsurface of shell elements are shown in Figure 9. The maximum principal stresses on the RTS and the MTTS are equal to σ_{max} = 3,50 x 10^{-1} MPa and σ_{max} = 1,50 x 10^{-1} MPa, respectively; the minimum principal stresses on the RTS and the MTTS are equal to σ_{min} = -4,28 x 10^{-1} MPa and σ_{min} = -5,28 x 10^{-1} MPa, respectively; as well as the average values of tensile principal stresses are equal to σ_{ave} = 4,00 x 10^{-8} MPa and σ_{ave} = 2,65 x 10^{-8} MPa, respectively.

It is worth noting that, also in this simulation, a relevant reduction of the maximum tensile principal stresses (56 %) can be obtained by considering the MTTS as an alternative configuration to the RTS.

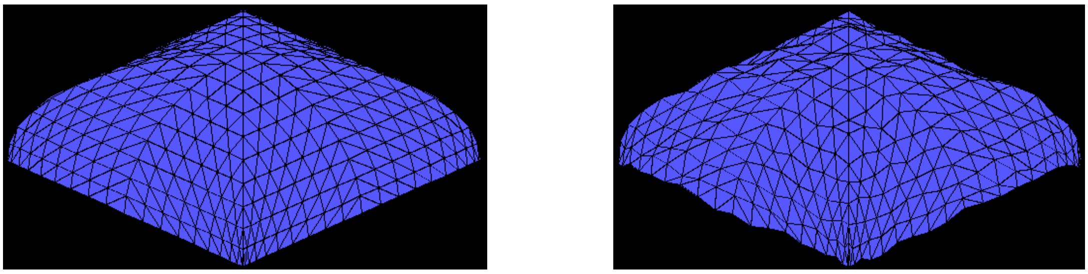

Figure 8: RTS and MTTS configurations.

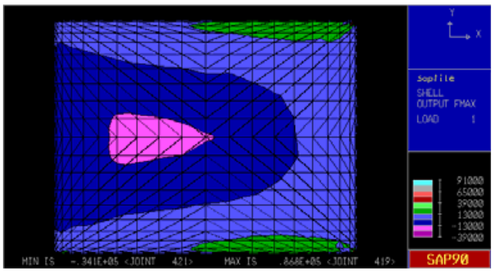

RTS: maximum principal internal forces [N/m]

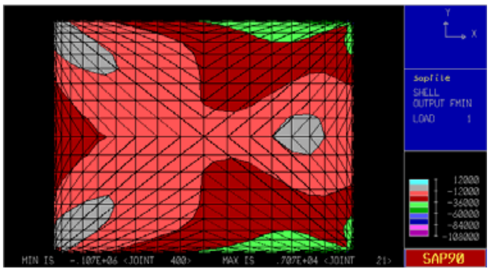

RTS: minimum principal internal forces [N/m]

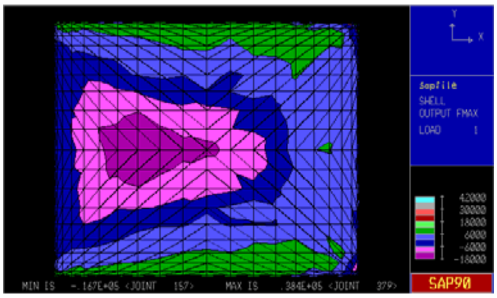

MTTS: maximum principal internal forces [N/m]

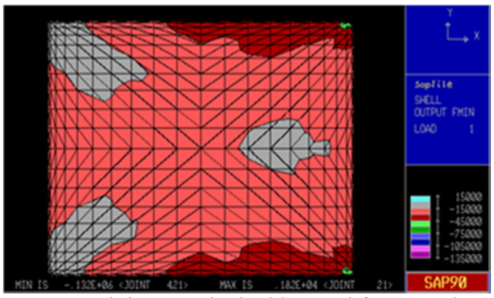

MTTS: minimum principal internal forces [N/m]

Figure 9: Top views of the unreinforced vault subject to seismic loads.

The FEM analysis on the MTTS has highlight, close to the vault basis, the principal tensile stresses are comparable to the tensile strength of tuff masonry (1,00 x 10^{-1} MPa) and the corresponding principal directions are roughly horizontal.

Therefore, a strengthening intervention with external unidirectional FRCM strips (Figure 10) is proposed. The mechanical properties of the used composites are given in Table 2.

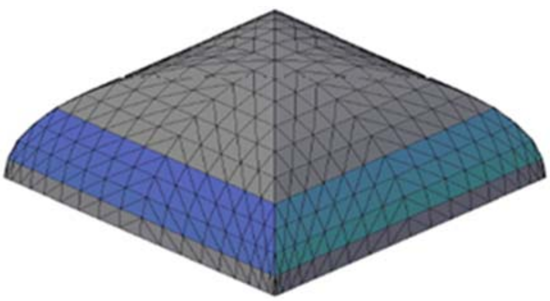

Figure 10: 3D views of the reinforced vault (the FRCM strips are applied on the blue surface).

Carbon fiber		Cementitious Matrix	
Tensile strenght	4800 MPa	Compressive strenght	≥ 20.0 MPa (after 28 d)
Young modulus	240 GPa	Flexural strenght	≥ 3.5 MPa (after 28 d)
Density	1.82 g/cm^3	Young modulus	≥ 7000 MPa (after 28 d)
Ultimate strain	1.8 %		

Table 2: Mechanical properties of FRCM.

The composites are assumed to be effective under pre-existing loads by applying a pretension in the strips via mechanical anchoring devices. The debonding failure modes and the composite bucking phenomena [24]-[36] can not occur in the strengthened vault, due to the use of such devices and the selective application of the FRCMs in correspondence with the vault regions subject to tensile stresses. The fiber orientation of the FRCMs is assumed to be parallel to the vault basis.

4 CONCLUDING REMARKS

An advanced numerical model able to approach the equilibrium problem of unreinforced and reinforced masonry vaults has been shown. This model allows to approximate the no-tension membrane (thrust surface) behavior of masonry through an elastic analysis of the masonry referred to a Minimum Tension Thrust Surface. Such a surface is obtained via a r-adaptive finite element featuring linearly elastic shell elements with dominant membrane behavior. The moving of the FEM nodes is governed by a Breeder Genetic Algorithm within a design domain and minimizing the average value of the principal tensile stresses in unreinforced masonry.

A cloister vault subject to several load combinations, both static and dynamic, has been studied in depth. The proposed model applied on the Minimum Tension Thrust Surface have given the tensile stresses significantly smaller than that obtained by means of the FEM analysis on the midsurface of the vault. The vulnerable portions of the vault have been found by means of the proposed model and a selective and optimized FRCM reinforcement has been designed.

The proposed approach may represent a useful tool to evaluate the vulnerability of existing curved masonry structures and to design optimal reinforcement patterns.

We address future extensions of the methodology here proposed to strengthening techniques involving a large variety of composite materials [69]-[76].

REFERENCES

[1] F. Fraternali, G. Bilotti, Non-Linear Elastic Stress Analysis in Curved Composite Beams. *Computers & Structures*, **62**, 837-869, 1997.

[2] F. Fraternali, Free Discontinuity Finite element models in two-dimensions for in-plane crack problems*, Theoretical and Applied Fracture Mechanics*, **47**, 274-282, 2007.

[3] F. Fraternali, C.D Lorenz, G. Marcelli, On the estimation of the curvatures and bending rigidity of membrane networks via a local maximum-entropy approach, *Journal of Computational Physics*, **231**, 528-540, 2012.

[4] A. Fortunato, F. Fraternali, M. Angelillo, Structural capacity of masonry walls under horizontal loads. *Ingegneria sismica N1, 41-51 Anno XXXI*, 2014.

[5] V.P. Berardi, Initiation of Failure for Masonry Subject to In-Plane Loads through Micromechanics. *Modelling and Simulation in Engineering*, 2016.

[6] J. Heyman, *The stone skeleton*. New York: Cambridge University Press; 1995.

[7] F. Fraternali, A. Marino, T. El Sayed, A. Della Cioppa, On the Structural Shape Optimization through Variational Methods and Evolutionary Algorithms. *Mechanics of Advanced Materials and Structure,* **18**, 225-243, 2011.

[8] A. Baratta, O. Corbi, On the statics of No-Tension masonry-like vaults and shells: Solution domains, operative treatment and numerical validation. *Annals of Solid and Structural Mechanics* **2**, 107, 2011.

[9] A. Baratta, O. Corbi, An approach to the positioning of FRP provisions in vaulted masonry structures. *Composites Part B Engineering,* **53**, 334-341, 2013.

[10] G. Carpentieri, F. Fabbrocino, M. De Piano, V.P. Berardi, L. Feo, F. Fraternali, Minimal mass design of strengthening techniques for planar and curved masonry structures. *7th European Congress on Computational Methods in Applied Sciences and Engineering*, (ECCOMAS 2016), Chania, Crete, Greece, June 5-10, 2016.

[11] F. Fraternali, A. Angelillo, F. Fortunato, A lumped stress method for plane elastic problems and the discrete-continuum approximation. *International Journal of Solids and Structures,* **39**, 6211-6240, 2002.

[12] F. Fraternali, A thrust network approach to the equilibrium problem of unreinforced masonry vaults via polyhedral stress functions. *Mechanics Research Communications*, **37**, 198-204, 2010.

[13] L. Soveja, M. Budescu, I. Gosav, *Modelling methods for unreinforced masonry structures*. Construction architecture. Gheorghe Asachi Technical University of Iai; LIX (LXIII), 2013.

[14] F. Fraternali, A mixed lumped stress-displacement approach to the elastic problem of masonry walls. *Mechanics Research Communications*, **38**, 176-180, 2011.

[15] M. Angelillo, A. Fortunato, A. Montanino, M. Lippiello, Singular stress fields in masonry structures: Derand was right. *Meccanica*, **49**, 1243-1262, 2014

[16] W.M. Jenkins, Plane frame optimum design environment based on genetic algorithm. *Journal of Structural Engineering, ASCE* **118**, 1992.

[17] P. Hajela, E. Lee, C.Y. Lin, Genetic algorithms in structural topology optimization. Mota Soares CA, Bendsøe MP, editors. *Topology design of structures, Vol. 227*. Dordrecht: Kluwer Academic Publishers, 1990.

[18] C.D. Chapman, K. Saitou, M.J. Jakiela, Genetic algorithms as an approach to configuration and topology design. *Journal Mechanical Design*, **116**, 1005-1012, 1994.

[19] K. DeJong, Evolutionary computation: a unified approach. *Genetic and Evolutionary Computation Conference (GECCO 2007)*, England UK, London, July 7-11, 2007.

[20] F. Fabbrocino, I. Farina, V.P. Berardi, A.J.M. Ferreira, F. Fraternali, On the thrust surface of unreinforced and FRP-/FRCM-reinforced masonry domes. *Composites Part B Engineering,* **83**,297-305, 2015.

[21] C. Maenghyo, J. Seongki, R-Adaptive mesh generation for shell finite element analysis, *Journal of Computational Physics,* **199**, 29-16, 2004.

[22] H. Mühlenbein, M. Schomisch, J. Born, The parallel genetic algorithm as function optimizer. *Parallel Computing*, **17**, 619-632, 1991.

[23] *European Committee for Standardization. Eurocode* 8: *Design of structures for earthquake resistance* - part 1: general rules, seismic actions and rules for buildings 2004. EN 1998-1. 2004. Brussels, Belgium.

[24] L. Ascione, F. Fraternali, A penalty model for the analysis of composite curved beams, *Computers & Structures*, **45**, 985-999, 1992.

[25] F. Fraternali, J.N. Reddy, A penalty model for the analysis of laminated composite shells, *International Journal of Solids and Structures*, **30**, 3337-3355, 1993.

[26] Ascione, L., V.P. Berardi, E. Di Nardo, L. Feo, G. Mancusi, An experimental and numerical investigation on the plating of reinforced concrete beams with FRP laminates. Lecture Notes in Applied and Computational Mechanics, 23, 303-314, 2005.

[27] Ascione, L., L. Feo, G. Mancusi, On the statical behaviour of fibre-reinforced polymer thin-walled beams. *Composites Part B: Engineering*, *31* (8), 643-654, 2000.

[28] L. Ascione, V.P. Berardi, L. Feo, G. Mancusi, A numerical evaluation of the interlaminar stress state in externally FRP plated RC beams. *Composites Part B: Engineering*, **36** (1), 83-90, 2005.

[29] L. Feo, G. Mancusi, Modeling shear deformability of thin-walled composite beams with open cross-section. *Mechanics Research Communications*, **37** (3), 320-325, 2010.

[30] G. Mancusi, L. Feo, Non-linear pre-buckling behavior of shear deformable thin-walled composite beams with open cross-section. *Composites Part B: Engineering*, **47**, 379-390, 2013.

[31] F. Fraternali, S. Spadea, L. Ascione, Buckling behavior of curved composite beams with different elastic response in tension and compression. *Composite Structures*, **100**, 280-289, 2013.

[32] G. Mancusi, F. Ascione, M. Lamberti, Pre-buckling behavior of composite beams: A mechanical innovative approach, *Composite Structures*, **117** (1), 396-410, 2014.

[33] L. Ascione, V.P. Berardi, Anchorage device for FRP laminates in the strengthening of concrete structures close to beam-column joints. *Composites Part B: Engineering*, **42** (7), 1840-1850, 2011

[34] L. Feo, G. Mancusi, The influence of the shear deformations on the local stress state of pultruded composite profiles. *Mechanics Research Communications*, **47**, 44-49, 2013.

[35] G. Mancusi, L. Feo, V.P. Berardi, Concrete open-wall systems wrapped with FRP under torsional loads. *Materials*, **5** (11), 2055-2068, 2012.

[36] L. Ascione, G. Mancusi, A. D'Aponte, Fabric-Reinforced Cementitious Matrix (FRCM): A new Italian guideline under development, *Key Engineering Materials*, **624**, 3-10, 2015.

[37] A. Amendola, G. Carpentieri, M. De Oliveira, R.E. Skelton, F. Fraternali, Experimental investigation of the softening-stiffening response of tensegrity prisms under compressive loading. *Composite Structures*, **117**, 234-243, 2014.

[38] A. Amendola, E.H. Nava, R. Goodall, I. Todd, R.E. Skelton, F. Fraternali, On the additive manufacturing, post-tensioning and testing of bi-material tensegrity structures, *Composite Structures*, **131**, 66-71, 2015.

[39] R.E. Skelton, F. Fraternali, G. Carpentieri, A. Micheletti, Minimum mass design of tensegrity bridges with parametric architecture and multiscale complexity. *Mechanics Research Communications*, 58, 124-132, 2014.

[40] A. Leonard, F. Fraternali, C. Daraio, Directional wave propagation in a highly nonlinear square packing of spheres. *Experimental Mechanics*, **53**(3), 327-337, 2013.

[41] F. Fraternali, G. Carpentieri, A. Amendola, R.E. Skelton, V. F. Nesterenko, Multiscale tunability of solitary wave dynamics in tensegrity metamaterials. *Applied Physics Letters*, **105**, 201903, 2014.

[42] J.R. Raney, F. Fraternali, A. Amendola, C. Daraio, Modeling and In Situ Identification of Material Parameters for Layered Structures based on Carbon Nanotube Arrays. *Composite Structures*, **93**, 3013–3018, 2011.

[43] F. Fraternali, I. Farina, C. Polzone, E. Pagliuca, L. Feo, On the use of R-PET strips for the reinforcement of cement mortars. *Composites. Part B*, **46**, 207-210, 2013.

[44] C. Daraio, D . Ngo, V. F. Nesterenko, F. Fraternali, Highly Nonlinear Pulse Splitting and Recombination in a Two Dimensional Granular Network. *Physical Review E*, **82**, 036603, 2010.

[45] A. Amendola, C.J. Smith, R. Goodall, F. Auricchio, L. Feo, G. Benzoni, F. Fraternali, Experimental response of additively manufactured metallic pentamode materials confined between stiffening plates. *Composite Structures*, **142**, 254-262, 2016.

[46] F. Fraternali, S. Spadea, V.P. Berardi, Effects of recycled PET fibers on the mechanical properties and seawater curing of Portland cement-based concretes. *Construction and Building Materials*, **61**, 293-302, 2014.

[47] I. Farina, F. Fabbrocino, G. Carpentieri, M. Modano, A. Amendola, R. Goodall, L. Feo, F. Fraternali, On the reinforcement of cement mortars through 3D printed polymeric and metallic fibers*, Composites Part B: Engineering*, **90**, 76-85, 2016.

[48] T. Blesgen, F. Fraternali, J.R. Raney, A. Amendola, C. Daraio, Continuum Limits of Bistable Spring Models of Carbon Nanotube Arrays accounting for Material Damage. *Mechanics Research Communications*, **45**, 58-63, 2012.

[49] F. Fraternali, M. Negri, M. Ortiz, On the Convergence of 3D Free Discontinuity Models in Variational Fracture. *International Journal of Fracture*, **166**(1-2), 3-11, 2010.

[50] Amendola, C.J. Smith, R. Goodall, F. Auricchio, L. Feo, G. Benzoni, F. Fraternali, Experimental response of additively manufactured metallic pentamode materials confined between stiffening plates. *Composite Structures*, **142**, 254–262, 2016.

[51] G. Lomiento , N. Bonessio, G. Benzoni, Friction Model for Sliding Bearings under Seismic Excitation, Journal of Earthquake Engineering, **17**(8):1162-1191, 2013..

[52] M. Budek, M. J. N. Priestley, G. Benzoni, The Effect of External Confinement on Flexural Hinging in Drilled Pile Shafts, *Earthquake Spectra*, **20** (1), 1-24, 2004.

[53] Hae-Bum Yun, Sami F. Masri, Raymond W. Wolfe, Gianmario Benzoni , Data-driven methodologies for change detection in large-scale nonlinear dampers with noisy measurements, *Journal of Sound and Vibration*, **322**, Issues 1–2, 24 April 2009, Pages 336–357.

[54] D. D'Ayala, G. Benzoni, Historic and Traditional Structures during the 2010 Chile Earthquake: Observations, Codes, and Conservation Strategies. *Earthquake Spectra*, **28** (S1), S425-S451, 2012.

[55] N. Bonessio, G. Lomiento, G. Benzoni, Damage identification procedure for seismically isolated bridges, *Structural Control Health Monitoring*, **19**(5), 565–578, 2012.

[56] G. Benzoni, C. Casarotti , Effects of Vertical Load, Strain Rate and Cycling on the Response of Lead-Rubber Seismic Isolators, *Journal of Earthquake Engineering* ,**13**, 2009.

[57] A. Budek-Schmeisser, G. Benzoni, Rational seismic design of precast, prestressed concrete piles, *PCI Journal*, **53**(5), 40-53, 2008.

[58] G. Benzoni, M. J. N. Priestley, Seismic response of linked marginal wharf segments, *Journal of Earthquake Engineering* **74**, 513-539, 2003.

[59] A. Amendola, G. Benzoni, F. Fraternali, Non-linear elastic response of layered structures, alternating pentamode lattices and confinement plates. *Composite Part B, Engineering*, Online first, DOI: 10.1016/j.compositesb.2016.10.027, 2016.

[60] F. Fraternali, G. Carpentieri, R. Montuori, A. Amendola, G. Benzoni, On the use of mechanical metamaterials for innovative seismic isolation systems, COMPDYN 2015 - 5th ECCOMAS Thematic Conference on Computational Methods in Structural Dynamics and Earthquake Engineering, 349-358.

[61] G. Mancusi, F. Fabbrocino, L. Feo, F. Fraternali, Size effect and dynamic properties of 2D lattice materials, *Composites Part B: Engineering*, **112**, 235-242, 2017.

[62] G. Mancusi, L. Feo, A refined finite element formulation for the microstructure-dependent analysis of two-dimensional (2D) lattice materials, *Materials*, **6** (1), 1-17, 2013.

[63] F. Ascione, G. Mancusi, Failure criteria for FRP adhesive lap joints: A comparative analysis. *Mechanics of Advanced Materials and Structures*, **17** (2), 157-164, 2010.

[64] F. Ascione, G. Mancusi, Axial/bending coupled analysis for FRP adhesive lap joints. *Mechanics of Advanced Materials and Structures*, *17* (2), 85-98,2010.

[65] F. Ascione, G. Mancusi, Curve adhesive joints. *Composite Structures*, **94** (8), 2657-2664, 2012.

[66] F. Ascione, G. Mancusi, The influence of the geometric curvature on the mechanical behaviour of the adhesive joint, *Civil-Comp Proceedings*, 99, 2012.

[67] G. Mancusi, F. Ascione. Performance at collapse of adhesive bonding. Composite Structures, **96**, 256-261, 2013.

[68] F. Ascione, G. Mancusi, The influence of the web-flange junction stiffness on the mechanical behaviour of thin-walled pultruded beams. *Composites Part B: Engineering*, **55**, 599-606, 2013.

[69] F. Ascione, G. Mancusi, S. Spadea, M. Lamberti, F. Lebon, A. Maurel-Pantel, On the flexural behaviour of GFRP beams obtained by bonding simple panels: An experimental investigation. *Composite Structures*, **131**, 55-65, 2015.

[70] G. Mancusi, A. Orefice, L. Feo, F. Fraternali, Structural analysis of adhesive bonding for thick-walled tubular composite profiles. *ECCOMAS Congress 2016 - Proceedings of the 7th European Congress on Computational Methods in Applied Sciences and Engineering*, **4**, 7837-7852, 2016.

[71] A. Orefice, G. Mancusi, L. Feo, F. Fraternali, Cohesive interface behaviour and local shear strains in axially loaded composite annular tubes. *Composite Structures*, 160, 1126-1135, 2017.

[72] Ascione, L., G. Mancusi, S. Spadea, Flexural behaviour of concrete beams reinforced with GFRP bars. *Strain*, **46** (5), 460-469, 2010.

[73] F. Ascione, G. Mancusi, An experimental analysis on the time-dependent behaviour of a CFRP retrofitting under sustained loads. *Proceedings of the 6th International Conference on Fracture Mechanics of Concrete and Concrete Structures*, **2**, 1085-1090, 2007.

[74] V.P. Berardi, G. Mancusi, Time-dependent behavior of reinforced polymer concrete columns under eccentric axial loading. *Materials*, **5** (11), 2342-235, 2012.

[75] V.P. Berardi, G. Mancusi, A mechanical model for predicting the long term behavior of reinforced polymer concretes, *Mechanics Research Communications*, **50**, 1-7, 2013.

[76] G. Mancusi, S. Spadea, V.P. Berardi, Experimental analysis on the time-dependent bonding of FRP laminates under sustained loads. *Composites Part B: Engineering*, **46**, 116-122, 2013.